Antagonism of CD317 Restriction of Human Immunodeficiency Virus Type 1 (HIV-1) Particle Release and Depletion of CD317 Are Separable Activities of HIV-1 Vpu[▽]

Christine Goffinet, Stefanie Homann, Ina Ambiel, Nadine Tibroni, Daniel Rupp,
Oliver T. Keppler,* and Oliver T. Fackler*

*Department of Infectious Diseases, Virology, University of Heidelberg, Im Neuenheimer Feld 324,
69120 Heidelberg, Germany*

Vpu antagonizes human immunodeficiency virus type 1 (HIV-1) particle release inhibition by CD317/BST-2/Tetherin. Whether this Vpu activity strictly requires cellular depletion of the restriction factor is unclear. Here, we characterized CD317 variants with mutations in putative sorting or ubiquitination motifs. All mutants still potently impaired release of Vpu-defective HIV-1 and remained sensitive to Vpu-mediated release enhancement. Importantly, this virological antagonism correlated with surface downregulation of CD317 mutants by Vpu, while intracellular pools of these mutants, which were consistently depleted of the wild-type protein, were highly variable or even enhanced. Thus, Vpu can efficiently antagonize virion tethering in the absence of CD317 degradation.

CD317 (BST-2/Tetherin/HM1.24) is an alpha interferon-inducible antiviral restriction factor that impairs the release of many enveloped viruses, including human immunodeficiency virus type 1 (HIV-1), HIV-2, and simian immunodeficiency virus (SIV), other retroviruses (9, 17), Lassa virus-like particles (VLPs) (21), and Marburg and Ebola VLPs (9, 10, 21). In the context of HIV-1, CD317 induces the retention (tethering) of mature particles at the producer cell surface and their subsequent internalization, thus preventing efficient release (17, 22). The HIV-1 accessory protein Vpu overcomes this restriction (17, 22), yet the underlying mechanism is not well understood; however, it may involve effects of Vpu on CD317, such as targeting to proteasomal and/or endolysosomal degradation or reducing its cell surface exposure (1, 4, 6, 7, 11, 15).

Reasoning that these processes may depend on intracellular sorting of CD317, we scanned the CD317 cytoplasmic tail (CT) for putative sorting and ubiquitination motifs (Fig. 1A). Three candidate motifs were identified: two lysines (K18 and K21) that might serve as ubiquitin acceptors (12), two leucines (L22 and L23) at the predicted junction of the CT and the transmembrane (TM) domain that might constitute a dileucine-based sorting signal, and a noncanonical tyrosine-based internalization motif (Y6 and Y8) that was recently reported to mediate endocytosis of CD317 from the cell surface (13, 19). We generated a set of CD317 mutants, with or without an N-terminal hemagglutinin (HA) tag, that bear changes of these motifs to alanine (Fig. 1A) and investigated them first regarding their ability to inhibit virus release. 293T cells were co-transfected with 1.2 μg of pHIV-1Δvpu proviral plasmid DNA and 0.1 μg of the indicated expression plasmid for CD317. Forty-eight hours posttransfection, cell culture supernatants were subjected to titration of infectious HIV-1 on TZM-bl reporter cells (4). Wild-type (WT) CD317 expression resulted in an approximately 100-fold reduction in the release of infectious HIV-1 Δvpu (Fig. 1B and D). Importantly, the CD317 mutants exerted comparable degrees of HIV-1 release inhibition. Concordant Western blot analyses of lysates of the virus-producing cells confirmed comparable cell-associated levels of p24CA in these samples and similar expression levels of all tagged and untagged CD317 variants tested (Fig. 1C and E). All CD317 variants displayed a characteristic band pattern between 20 to 35 kDa, reflecting differential glycosylation (4, 17). Similar to chimeras of the human and rodent CD317 proteins (4), the protein pattern seen for the CD317 mutant with K18A and K21A mutations [K(18,21)A] suggested that the relative intensity of these bands is not predictive of CD317's antiviral potency or Vpu sensitivity. Irrespective of the presence of the epitope tag, detection of CD317 by an anti-CD317 antibody (16) revealed additional low- and high-molecular-weight CD317 species that presumably reflect unglycosylated and multimeric forms of the restriction factor, respectively (Fig. 1C and E, upper panels) (2, 18). These species were poorly detected by an antibody targeting the N-terminal HA tag (Fig. 1C, anti-HA). Immunofluorescence analysis for the subcellular localization of HA-CD317 by using an anti-HA antibody showed a marked intracellular distribution for all variants that was comparable to that described before for HA-WT CD317 (Fig. 1F, anti-HA) (4). In stark contrast, all untagged CD317 variants were predominantly found at the cell surface when detected with the anti-CD317 antibody (Fig. 1G). Of particular note, this seeming difference in localization simply reflected altered accessibility of the epitopes used for antibody recognition at the plasma and intracellular membranes: staining of all HA-CD317 variants with
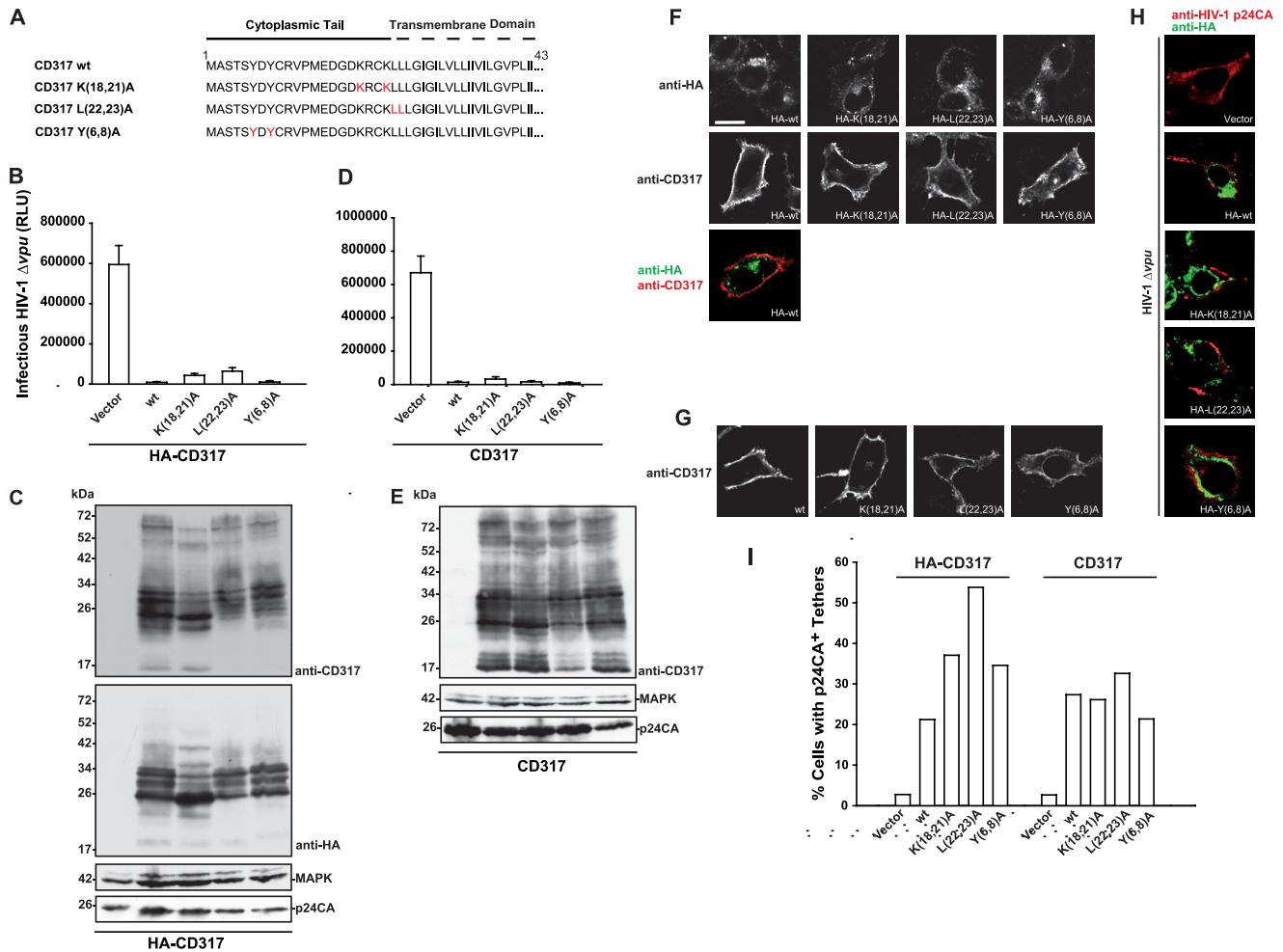
FIG. 1. Characterization of basic properties of CD317 CT mutants. (A) Amino acid alignment of CD317 and CD317 CT mutants. (B and D) Released infectivity of 293T cells transfected with pHIV-1Δvpu and expression constructs for HA-tagged (B) or untagged (D) CD317. RLU, relative light units. Arithmetic means ± standard deviations (SD) of one experiment performed in triplicate are given. (C and E) Western blot analyses of corresponding 293T cell lysates. CD317 was detected using a polyclonal anti-CD317 antibody recognizing the extracellular domain of CD317 (16). MAPK, mitogen-activated protein kinase. (F) 293T cells grown on coverslips were transfected with expression plasmids for the indicated HA-CD317 variants. Presented are confocal micrographs for the localization of HA-CD317 proteins by using an anti-HA antibody (upper panels) or the polyclonal anti-CD317 antibody (middle panels). The bottom panel depicts a merge picture of a double staining of a 293T cell expressing HA-WT CD317 with anti-HA and anti-CD317 antibodies. Scale bar, 10 μm. (G) Micrographs of 293T cells expressing the indicated CD317 variants following staining with anti-CD317 antibody. (H) 293T cells transfected with pHIV-1Δvpu and the indicated HA-CD317 proteins were stained for HIV-1 p24CA (red) and HA-CD317 (green). (I) Quantification of p24CA/HA-CD317 double-positive cells showing virus tethering (Gag accumulation at the surface and/or Gag internalization), essentially as previously reported (4).

the anti-CD317 antibody revealed the same cell surface localization as that of the corresponding untagged proteins (Fig. 1F, anti-CD317; see bottom panel for simultaneous detection of cell surface and intracellular pools of HA-WT CD317). Thus, neither epitope tagging nor the CT mutations affected the steady-state subcellular distribution of CD317.

We next addressed the abilities of the CD317 mutants to induce cell surface virion tethering by immunofluorescence analysis of 293T cells that were treated as described for the experiment whose results are shown in Fig. 1B to E. In the absence of CD317, p24CA staining was diffuse throughout the cytoplasm (Fig. 1H). Expectedly (4, 17), HA-WT CD317 expression led to a pronounced redistribution of p24CA, resulting in the frequent formation of aggregates at the plasma membrane and intracellularly (quantification is shown in Fig.

1I). Notably, virion tetherings of similar appearances and potencies were observed in the presence of all CD317 mutants analyzed, and the magnitude of virion tethering was only slightly affected by the presence of the HA tag. Together, these results reveal that putative sorting motifs in the CD317 CT do not govern the restriction factor's ability to interfere with HIV-1 particle release.

Next, we examined whether mutations in the CD317 CT might alter sensitivity of the restriction factor to Vpu antagonism. Proviral plasmids encoding either WT HIV-1 or the isogenic HIV-1 Δvpu were cotransfected into 293T cells with increasing amounts of CD317-encoding constructs (Fig. 2). Quantification of the amounts of infectious HIV-1 released 48 h posttransfection revealed the established pattern of Vpu-mediated antagonism of HA-CD317: high levels of the restric-
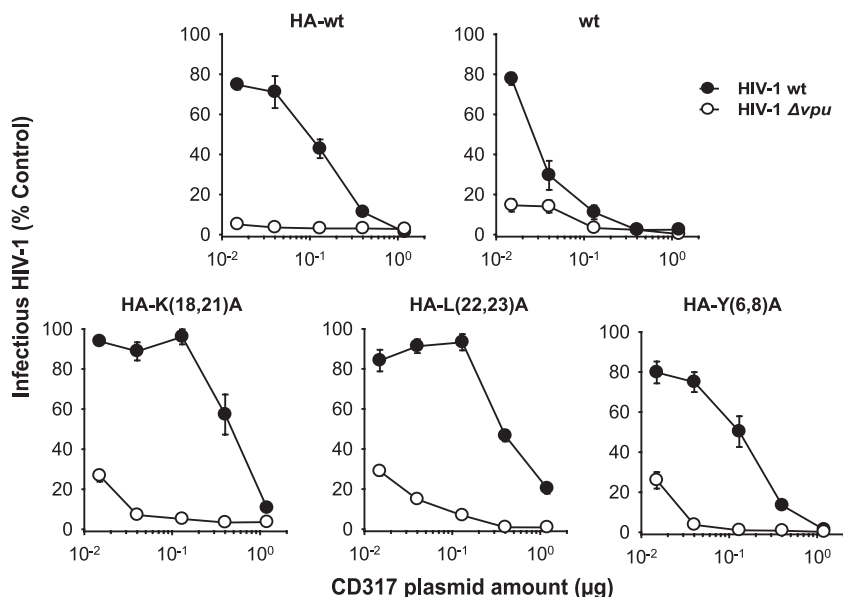
FIG. 2. Dose titration analysis for WT and mutant CD317 in cells coexpressing WT or Vpu-defective HIV-1. Titration of plasmids encoding HA-CD317, CD317, or CT mutants of HA-CD317 in 293T cells cotransfected with either pHIV-1 wt or pHIV-1Δ*vpu*. Culture supernatants were analyzed for the yield of infectious HIV-1 two days posttransfection. Shown are the levels of infectious secreted virus relative to WT HIV-1 in the absence of CD317 (empty vector, set to 100%). Values depicted are the arithmetic means of triplicates ± SD from one experiment representative of two experiments.

tion factor potently inhibited both WT HIV-1 and HIV-1 Δ*vpu* particle release, whereas medium to low levels of CD317 were susceptible to Vpu counteraction, allowing efficient release of infectious virus progeny. Epitope tagging did not exert significant effects on the antiviral activity of WT CD317 (Fig. 2, upper panels). Importantly, this concentration- and Vpu-dependent HIV-1 release pattern was preserved for all HA-CD317 mutants. Of note, the three mutants appeared to be slightly less potent at the lowest expression levels. These results suggest that none of the putative sorting motifs in the CD317 CT is essential for Vpu sensitivity.

To examine whether this Vpu-mediated rescue correlated with the depletion of CD317, we cotransfected 293T cells with HIV-1 proviral DNA and moderate amounts of WT or K(18,21)A CD317 (100 ng), an experimental condition that recapitulates the Vpu-sensitive block of particle release (Fig. 3A). Western blot analyses of lysates from these virus-producing cells demonstrated an epitope tag-independent and significant reduction of WT CD317 protein amounts in the presence of Vpu, as reported previously (Fig. 3C and D) (4). Conversely, steady-state levels of K(18,21)A CD317 were completely refractory to Vpu-induced depletion, despite efficient Vpu-mediated release enhancement. Pulse-chase metabolic labeling experiments confirmed that provirally expressed Vpu reduces the stability of HA-WT CD317 (Fig. 3E and F) (4). In contrast, HA-K(18,21)A CD317 was slightly less stable than WT CD317 in the absence of Vpu, but its half-life was not affected by the presence of Vpu. This lack of correlation between Vpu-induced CD317 depletion and rescue of virion release was confirmed in a series of steady-state analyses (analogous to those shown in Fig. 3A to D) including all four HA-CD317 constructs (Fig. 3G contains a summary of CD317 expression levels as a function of the Vpu-mediated release enhance-

ment). While steady-state levels of HA-WT CD317 were reduced, HA-K(18,21)A CD317 expression was unchanged or even slightly elevated in the presence of Vpu in all experiments performed. For unknown reasons, expression levels of HA-L(22,23)A CD317 and HA-Y(6,8)A CD317 proteins in response to Vpu displayed a considerable interexperimental variability. Importantly, irrespective of these fluctuations in steady-state expression, Vpu consistently and efficiently antagonized the virion release restriction imposed by all CD317 variants. In sum, lysine residues in the CD317 CT are determinants for Vpu-mediated depletion of CD317. This depletion, however, is dispensable for potent antagonism of the CD317-mediated restriction of HIV-1 particle release.

We then assessed the ability of Vpu to reduce cell surface exposure of WT and mutant CD317 proteins. 293T cells, all stably expressing HA-CD317 variants at comparable levels (data not shown), were infected with vesicular stomatitis virus (VSV) G-protein-pseudotyped WT or HIV-1 Δ*vpu* virions. Seventy-two hours postinfection, cells were consecutively stained for cell surface CD317 and intracellular p24CA. Parallel analysis of the infectious virus titers produced from infected 293T lines confirmed for all HA-CD317 variants marked inhibition of particle release and antagonism thereof in the absence and presence of Vpu, respectively (Fig. 4B). Expectedly (1, 4, 6, 15), Vpu induced an approximately 2-fold reduction in cell surface levels of HA-WT CD317 (Fig. 4A). Importantly, mutating the putative sorting and ubiquitination motifs in the CT had no effect on the sensitivity of HA-CD317 to Vpu-mediated downregulation from the cell surface. Thus, reduction of CD317 cell surface exposure correlates with the antagonistic activity of Vpu and is not coupled to depletion of intracellular CD317 pools.

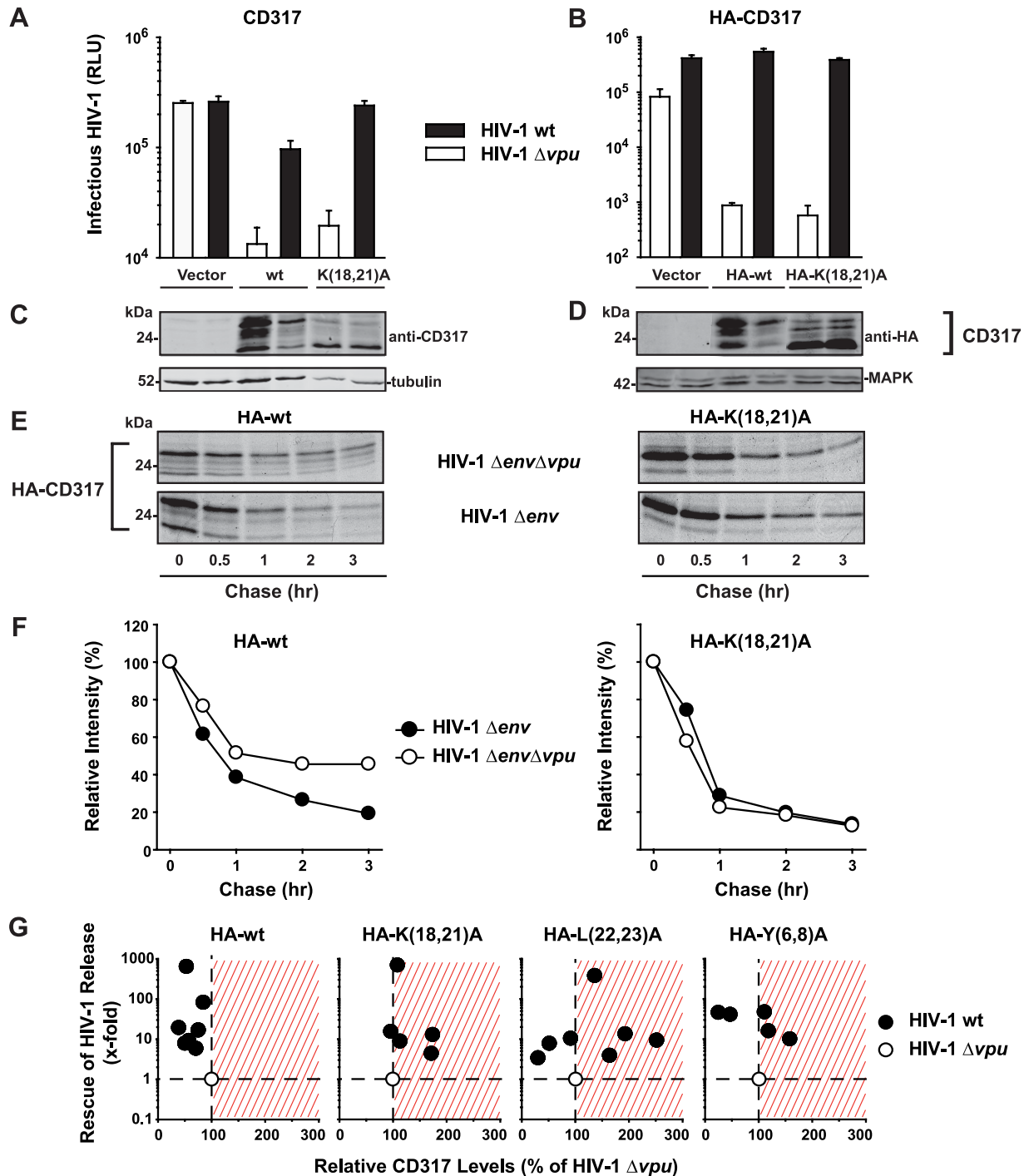Several recent studies identified molecular determinants in

FIG. 3. Effects of provirally encoded Vpu on the WT and mutant HA-CD317-imposed restrictions of HIV-1 release and on HA-CD317 protein levels. Histogram bars show the levels of infectious virus secreted from 293T cells expressing either WT HIV-1 or HIV-1 Δ*vpu* and vector, CD317, or CD317 K(18,21)A (A) or vector, HA-CD317, or HA-CD317 K(18,21)A (B). Shown are arithmetic means ± SD of triplicates from one experiment representative of 5 to 7 experiments. (C and D) Western blot analyses of corresponding 293T cell lysates. (E) Pulse-chase radiolabeling. 293T cells transiently expressing HA-CD317 or mutants together with HIV-1 Δ*env* or HIV-1 Δ*env* Δ*vpu* were pulse-labeled with [³⁵S]methionine and then incubated with chase media for the indicated times (hours [hr]). After immunoprecipitation with anti-HA antibody, proteins were separated by SDS-PAGE and the gels were subjected to autoradiography as previously described (4). (F) The relative intensities of the HA-CD317 bands were quantified, and values at 0 h were set to 100% and graphed. Given are the results of one of two independent experiments. (G) 293T cells were transfected with pHIV-1 wt or pHIV-1Δ*vpu* and the indicated HA-CD317 expression constructs. Relative levels of HA-CD317 and MAPK protein in cell lysates were quantified by use of the Odyssey infrared imaging system and Odyssey software. The ratio of HA-CD317 to MAPK for HIV-1 Δ*vpu*-coexpressing cells was set to 100% (*x* axis). The *y* axis depicts the factor of titer enhancement of WT HIV-1 relative to the value for HIV-1 Δ*vpu*, the latter of which was set to 1 in each experiment. Each circle represents the result of one of 5 to 7 independent experiments.
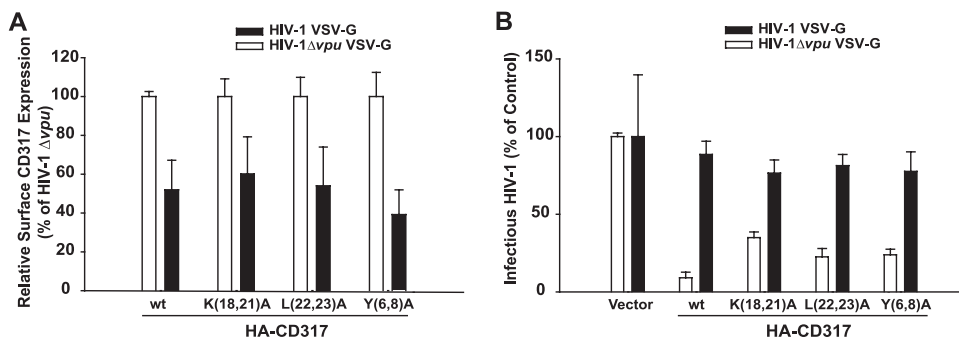
FIG. 4. Susceptibilities of WT and mutant CD317 proteins to Vpu-mediated downregulation from the cell surface upon HIV-1 infection. 293T cells stably expressing pcDNA3.1 (vector), WT HA-CD317, or HA-CD317 mutants were infected with VSV G-pseudotyped WT HIV-1 or HIV-1 Δ*vpu*. Seventy-two hours postinfection, cells were analyzed by flow cytometry using surface CD317 staining (anti-CD317 monoclonal antibody from Chugai Pharmaceuticals) to quantify HA-CD317 surface expression levels and concurrent intracellular p24CA staining to identify productively infected cells. Uninfected cells and HA-CD317-expressing cells infected in the presence of the reverse transcriptase inhibitor efavirenz (1 μM) served as negative controls (not shown). Values depicted are the arithmetic means of triplicates ± standard errors of the means from three independent experiments. (A) The relative cell surface expression levels of HA-CD317 and mutants are depicted, with values for the HIV-1 Δ*vpu*-infected cells set to 100%. (B) Quantification of infectious HIV-1 in the cell supernatant at the time of cell harvest for flow cytometry.

the CD317 TM domain that govern its sensitivity to Vpu (6, 14, 20). However, mutation of these determinants disrupted both rescue of HIV-1 particle release and depletion of cellular CD317. The generation of a CD317 mutant that is counteracted by Vpu in the absence of CD317 depletion thus provides the first genetic evidence that these two Vpu activities are separable. This finding is corroborated by the lack of (i) correlation between CD317 depletion and Vpu-mediated release restriction antagonism in the analysis of our set of CD317 mutants and (ii) CD317 depletion upon HIV-1 infection of certain T-lymphocyte lines, in which Vpu modestly facilitates HIV-1 particle release (16). Thus, similar to the activities of other viral CD317 antagonists (2, 8, 10, 23), Vpu's anti-CD317 antagonizing activity does not strictly depend on degradation of the restriction factor. Nevertheless, in the context of HIV-1 infection, Vpu efficiently depletes cellular CD317 pools in most T-lymphocyte lines as well as in primary macrophages (4, 16, 20), and blocking of Vpu-mediated CD317 degradation by the addition of proteasome inhibitors interferes with Vpu's antagonism to CD317 (4, 6, 11). Although indirect effects of the proteasome inhibitors used in these experiments cannot be excluded, these results suggest that the reduction of total cell-associated CD317 levels by Vpu can contribute to its function as a CD317 antagonist. Similar to the antagonism of APOBEC3G by HIV-1 Vif (5), Vpu may thus counteract CD317 by at least two independent mechanisms, only one of which involves depletion of the restriction factor. The data presented here are in line with a scenario in which the reduction of CD317 cell surface exposure by Vpu is instrumental for this degradation-independent functional antagonism. While the precise mechanism by which Vpu subverts endocytosis, recycling or other intracellular sorting steps of CD317, remains to be determined, this likely involves the sequestration of CD317 to the *trans*-Golgi network (3). Which mechanism is predominantly used by Vpu for CD317 antagonism is conceivably dictated by parameters such as CD317 and Vpu expression levels and/or the availability of specific degradation pathways in a given HIV target cell.

REFERENCES

1. **Bartee, E., A. McCormack, and K. Fruh.** 2006. Quantitative membrane proteomics reveals new cellular targets of viral immune modulators. PLoS Pathog. **2:**e107.
2. **Douglas, J. L., K. Viswanathan, M. N. McCarroll, J. K. Gustin, K. Fruh, and A. V. Moses.** 2009. Vpu directs the degradation of the human immunodeficiency virus restriction factor BST-2/Tetherin via a {beta}TrCP-dependent mechanism. J. Virol. **83:**7931–7947.
3. **Dubé, M., B. B. Roy, P. Guiot-Guillain, J. Mercier, J. Binette, G. Leung, and E. A. Cohen.** 2009. Suppression of Tetherin-restricting activity upon human immunodeficiency virus type 1 particle release correlates with localization of Vpu in the trans-Golgi network. J. Virol. **83:**4574–4590.
4. **Goffinet, C., I. Allespach, S. Homann, H. M. Tervo, A. Habermann, D. Rupp, L. Oberbremer, C. Kern, N. Tibroni, S. Welsch, J. Krijnse-Locker, G. Banting, H. G. Krausslich, O. T. Fackler, and O. T. Keppler.** 2009. HIV-1 antagonism of CD317 is species specific and involves Vpu-mediated proteasomal degradation of the restriction factor. Cell Host Microbe **5:**285–297.
5. **Goila-Gaur, R., and K. Strebel.** 2008. HIV-1 Vif, APOBEC, and intrinsic immunity. Retrovirology **5:**51.
6. **Gupta, R. K., S. Hue, T. Schaller, E. Verschoor, D. Pillay, and G. J. Towers.** 2009. Mutation of a single residue renders human tetherin resistant to HIV-1 Vpu-mediated depletion. PLoS Pathog. **5:**e1000443.
7. **Iwabu, Y., H. Fujita, M. Kinomoto, K. Kaneko, Y. Ishizaka, Y. Tanaka, T. Sata, and K. Tokunaga.** 2009. HIV-1 accessory protein Vpu internalizes cell-surface BST-2/tetherin through transmembrane interactions leading to lysosomes. J. Biol. Chem. **284:**35060–35072.
8. **Jia, B., R. Serra-Moreno, W. Neidermyer, A. Rahmberg, J. Mackey, I. B. Fofana, W. E. Johnson, S. Westmoreland, and D. T. Evans.** 2009. Species-specific activity of SIV Nef and HIV-1 Vpu in overcoming restriction by tetherin/BST2. PLoS Pathog. **5:**e1000429.
9. **Jouvenet, N., S. J. Neil, M. Zhadina, T. Zang, Z. Kratovac, Y. Lee, M. McNatt, T. Hatziioannou, and P. D. Bieniasz.** 2009. Broad-spectrum inhibition of retroviral and filoviral particle release by tetherin. J. Virol. **83:**1837–1844.
10. **Kaletsky, R. L., J. R. Francica, C. Agrawal-Gamse, and P. Bates.** 2009. Tetherin-mediated restriction of filovirus budding is antagonized by the Ebola glycoprotein. Proc. Natl. Acad. Sci. U. S. A. **106:**2886–2891.
11. **Mangeat, B., G. Gers-Huber, M. Lehmann, M. Zufferey, J. Luban, and V. Piguet.** 2009. HIV-1 Vpu neutralizes the antiviral factor Tetherin/BST-2 by binding it and directing its beta-TrCP2-dependent degradation. PLoS Pathog. **5:**e1000574.

12. **Mansouri, M., K. Viswanathan, J. L. Douglas, J. Hines, J. Gustin, A. V. Moses, and K. Fruh.** 2009. Molecular mechanism of BST2/tetherin down-regulation by K5/MIR2 of Kaposi's sarcoma-associated herpesvirus. J. Virol. **83:**9672–9681.

13. **Masuyama, N., T. Kuronita, R. Tanaka, T. Muto, Y. Hirota, A. Takigawa, H. Fujita, Y. Aso, J. Amano, and Y. Tanaka.** 2009. HM1.24 is internalized from lipid rafts by clathrin-mediated endocytosis through interaction with {alpha}-adaptin. J. Biol. Chem. **284:**15927–15941.

14. **McNatt, M. W., T. Zang, T. Hatziioannou, M. Bartlett, I. B. Fofana, W. E. Johnson, S. J. Neil, and P. D. Bieniasz.** 2009. Species-specific activity of HIV-1 Vpu and positive selection of tetherin transmembrane domain variants. PLoS Pathog. **5:**e1000300.

15. **Mitchell, R. S., C. Katsura, M. A. Skasko, K. Fitzpatrick, D. Lau, A. Ruiz, E. B. Stephens, F. Margottin-Goguet, R. Benarous, and J. C. Guatelli.** 2009. Vpu antagonizes BST-2-mediated restriction of HIV-1 release via beta-TrCP and endo-lysosomal trafficking. PLoS Pathog. **5:**e1000450.

16. **Miyagi, E., A. J. Andrew, S. Kao, and K. Strebel.** 2009. Vpu enhances HIV-1 virus release in the absence of Bst-2 cell surface down-modulation and intracellular depletion. Proc. Natl. Acad. Sci. U. S. A. **106:**2868–2873.

17. **Neil, S. J., T. Zang, and P. D. Bieniasz.** 2008. Tetherin inhibits retrovirus release and is antagonized by HIV-1 Vpu. Nature **451:**425–430.

18. **Perez-Caballero, D., T. Zang, A. Ebrahimi, M. W. McNatt, D. A. Gregory, M. C. Johnson, and P. D. Bieniasz.** 2009. Tetherin inhibits HIV-1 release by directly tethering virions to cells. Cell **139:**499–511.

19. **Rollason, R., V. Korolchuk, C. Hamilton, P. Schu, and G. Banting.** 2007. Clathrin-mediated endocytosis of a lipid-raft-associated protein is mediated through a dual tyrosine motif. J. Cell Sci. **120:**3850–3858.

20. **Rong, L., J. Zhang, J. Lu, Q. Pan, R. P. Lorgeoux, C. Aloysius, F. Guo, S. L. Liu, M. A. Wainberg, and C. Liang.** 2009. The transmembrane domain of BST-2 determines its sensitivity to down-modulation by human immunodeficiency virus type 1 Vpu. J. Virol. **83:**7536–7546.

21. **Sakuma, T., A. Sakurai, and J. Yasuda.** 2009. Dimerization of tetherin is not essential for its antiviral activity against Lassa and Marburg viruses. PLoS One **4:**e6934.

22. **Van Damme, N., D. Goff, C. Katsura, R. L. Jorgenson, R. Mitchell, M. C. Johnson, E. B. Stephens, and J. Guatelli.** 2008. The interferon-induced protein BST-2 restricts HIV-1 release and is downregulated from the cell surface by the viral Vpu protein. Cell Host Microbe **3:**245–252.

23. **Zhang, F., S. J. Wilson, W. C. Landford, B. Virgen, D. Gregory, M. C. Johnson, J. Munch, F. Kirchhoff, P. D. Bieniasz, and T. Hatziioannou.** 2009. Nef proteins from simian immunodeficiency viruses are tetherin antagonists. Cell Host Microbe **6:**54–67.